ACS OMEGA

Article

Cite This: ACS Omega 2019, 4, 8778−8785

http://pubs.acs.org/journal/acsodf

Fabrication of Poly(vinyl alcohol)/Chitosan/*Bidens pilosa* Composite Electrospun Nanofibers with Enhanced Antibacterial Activities

James Kegere,[†] Amged Ouf,[‡] Rania Siam,[‡] and Wael Mamdouh*[,†]

[†]Department of Chemistry, School of Sciences and Engineering (SSE) and [‡]Department of Biology and Biotechnology Graduate Program, School of Sciences and Engineering (SSE), The American University in Cairo (AUC), AUC Avenue, P.O. Box 74, New Cairo 11835, Egypt

Supporting Information

ABSTRACT: Due to the current challenges faced by the increasing rate of drug-resistant bacteria, attention is gradually shifting from synthetic antimicrobial chemical compounds to natural products that are ecofriendly with a wide spectrum of properties. The aim of this research was to successfully fabricate electrospun nanofibers from poly(vinyl alcohol) (PVA), PVA blended with *Bidens pilosa* and chitosan composite blends and investigate their potential antibacterial activities against *Escherichia coli* and *Staphylococcus aureus*. Fabrication of nanofibers was performed by the electrospinning technique, which applies high voltage on the polymer, forcing it to spin off as a jet onto a plate collector. Characterization of the nanofibers was successfully performed by scanning electron microscopy and Fourier transform infrared spectroscopy. Antibacterial assessment was carried out by colony forming unit enumeration. The results obtained revealed a 12% increase in growth inhibition of bacteria in composite nanofibers as compared with their parental forms, which were >91 and 79%, respectively. Chitosan nanofibers have been extensively researched, and their antibacterial properties have been studied. However *B. pilosa* antibacterial properties in a nanofiber form have not been previously reported. These composite nanofibers open new avenues toward using natural materials as potent antibacterial agents.

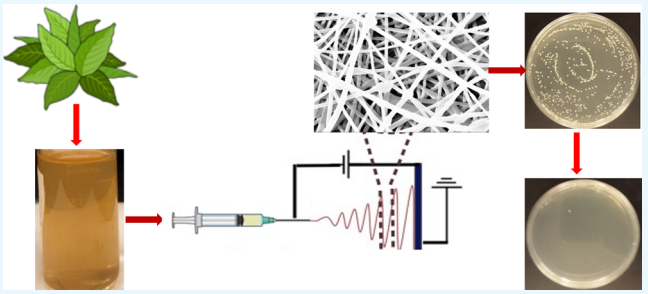

1. INTRODUCTION

Despite the modern technological advancements in biomedical research, disease outbreaks caused by bacterial infections continue to claim lives and cause uncertainty to humanity.[1,2] The rate of microbial resistance is rising dangerously around the world and endangering man, plants, and animals in equal measure. This threat has complicated the development of new conventional chemical compounds, resulting in the decline in research and development for new antibiotics.[2,3] Bacterial infection is a common occurrence in the world and especially in remote areas where modern medicare is hard to get.[4] The recent advances in nanotechnology have provided a modicum of hope to cope with the fears caused by looming bacterial outbreaks.[5] Materials at the nanoscale exhibit properties that are not seen or believed to exist in the bulk scale of the same materials.[6] Nanotechnology and nanomaterials have been in existence for long time, for example silver and silver nanoparticles were some of the first antimicrobial materials used extensively in the ancient world.[6,7] Until today, silver remains a potent antimicrobial agent that is commonly added to cosmetics and shampoos to prevent infections.[8] Although the newly discovered nanomaterials may have individual antibacterial properties, focus is now being switched to composite, biodegradable materials with synergistic effect against microbial infections.[9] Development of nanocomposites has been inspired by the challenges and limitations encountered when using microcomposites and monolithic materials.[8] Although they pose challenges in preparation due to the stoichiometric limitations in the nanophase, nanocomposites generally offer superior and user-friendly properties when compared with the microcomposites and monoliths.[4] Nanocomposite materials are reputed to be materials of the 21st century owing to uniqueness in property combinations, which are rarely found in conventional materials. Development of nanofibers and their applications in various fields have attracted tremendous attention from the scientific community in the last decade.[10,11] This is due to the unique novel properties that come with reduction in size toward the nanoscale, and for the case of fibers, it comes with myriad benefits in both environment and biomedical fields.[12] Nanofibers have a large surface-area−volume ratio, an easily biofunctionalized surface, and superior mechanical properties.[13] These properties have made nanofibers versatile in applications ranging from engineering to medical, environmental, and catalysis areas.[14]

Received: January 23, 2019
Accepted: May 10, 2019
Published: May 22, 2019

DOI: 10.1021/acsomega.9b00204
ACS Omega 2019, 4, 8778−8785

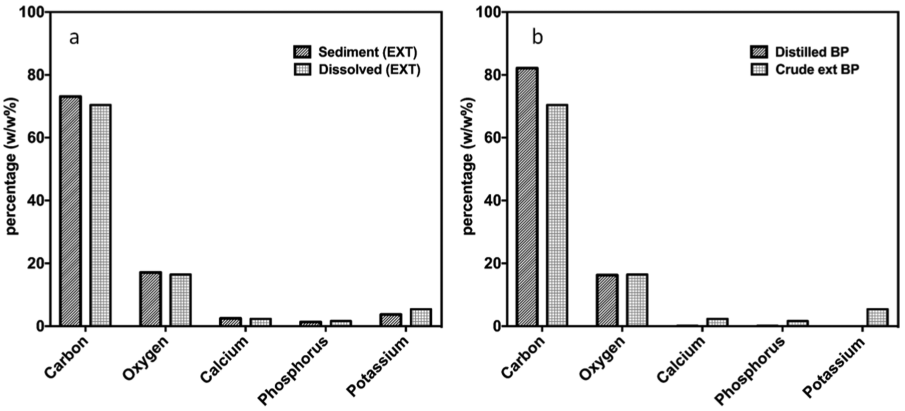

Figure 1. EDX analysis of elements present in (a) sediment and (b) dissolved PVA:EXT.

Electrospinning is a technique in which materials in a solution form are subjected to high-voltage power supply to produce fibers that are in the micro and nano size range. For the electrospinning process to occur, the following parameters have to be considered and carefully controlled: polymer solution, high voltage power supply, and the distance from the spinneret to the collector plate. The mechanism that leads to the formation of fibers herein is the stretching of the solution as it attempts to drop off the needle tip. This stretching is forced by the electrostatic forces that act on the polymer solution as a result of a repulsion between the polymer molecules and changes in the current. The solution is forced to pass through a narrow orifice electrified by the applied voltage in the range between 10 and 30 kV, which charges the solution and leads to the formation of a tailor cone, which then provides a platform for the jet of the material to whip down violently toward the collector plate.

The goal of this project was to synthesize poly(vinyl alcohol) (PVA)/*Bidens pilosa* (BP)/chitosan (CS) composite nanofibers and investigate the effect of solution electrospinning parameters on the fabrication of these nanocomposites and their antibacterial properties.

PVA is a well-known polymer because of its biocompatibility and biodegradability, and these novel qualities have made it gain enormous attention in biomedical research for multiple applications ranging from drug delivery to antibiotic development and scaffolds for tissue engineering applications.[15] Chitosan on the other hand is also known to have strong antibacterial activity against both Gram-positive and Gram-negative bacteria, viruses, and fungi.[16] It has attracted great attention over the last 2 decades in biomedical applications given the novelty chitosan has as pertains to its properties.[16] The mechanism of chitosan antibacterial action has been extensively studied, and previous research has linked the polycationic nature of the amine groups, in solution, to lowering the pH below 6.5.[17] The cations in the biopolymer are therefore believed to interact with the negative charges on the cell membrane of microorganisms, leading to the hydrolysis of the peptidoglycan and thus affecting the physiological processes of the cell.[18]

B. pilosa (BP) is a herbaceous plant commonly referred to as Spanish needle or black jack, originated in South America, and widely distributed around the world being used as a food and medicine in many communities in Africa, America, Asia, and Oceania.[19]

BP is a rich reservoir of phytochemicals, which give it unique properties useful in antimicrobial, antiseptic, anti-inflammatory, antioxidant, anticancer, and nutritional applications. Research conducted to profile the phytochemicals found in BP revealed that it contained about 201 compounds, of which 34.8% are aliphatic compounds, 29.8% terpenoids, 9.45% phenylpropanoids, 6.4%, aromatics, 3.9% porphyrins, and 2.9% other compounds.[19] Each part of the world has adopted BP for different functions, for example, in Africa, it is used for the treatment of wounds, diarrhea, influenza, headache, stomachache, etc.[19] In Cuba, the decoction (boiled extract) of BP is used as a juice as well as an anti-inflammatory agent and also in the treatment of diabetes and asthma. It is also used as a medicine for conjunctivitis, otitis, colic, and snakebites in China. In Central America, BP is important in the treatment of eye infections and is used as a diuretic and hypotensive agent. In Uganda, BP has been explored in the treatment of malaria, wounds, nasal bleeds, and stomach ulcers. The list of applications in the biomedical field is extensive.[19] Thus, in this work, the combination of PVA, chitosan, and BP extract, particularly in the nanofiber form, is expected to have a synergistic antimicrobial effect against different bacterial strains.

2. RESULTS AND DISCUSSION

2.1. Solubility and Miscibility of the Composites. In preparing PVA (polyvinyl alcohol):EXT (crude extract *B. pilosa*) and PVA:DBP (distilled *B. pilosa*) in situ and ex situ to be electrospun, care was taken to ensure that solution parameters were optimized to produce smooth nanofibers. PVA:DBP was completely solubilized, and formation of nanofibers was a smooth process. For PVA:EXT, about 90% of the extract was solubilized, while the undissolved/sediment portion accounted for 10%. Energy-dispersive X-ray spectroscopy (EDX) analysis of the sediment and solution of PVA:EXT revealed changes in the composition of carbon-based materials, oxygen groups, and minerals. Sediments contained slightly higher percentage of carbon and oxygen, meaning that derivatives of these elements were evenly distributed, as shown in Figure 1a. Generally the amount of minerals was more in the soluble portion than in the sediment as most of them were water-soluble. On the other hand, both distilled and crude extracts contained similar percentages of oxygen although they differed in the quantity of carbon and minerals, as can be seen in Figure 1b.

DOI: 10.1021/acsomega.9b00204
ACS Omega 2019, 4, 8778−8785

2.2. Effect of Working Parameters on the Properties of the Formed Nanofibers. Voltage was an important parameter for the electrospinning process and influenced to a great extent the morphological properties of the formed nanofibers. To be able to spin the solution in the syringe to obtain fibers, an optimum amount of the applied voltage is required to eject and sequester the liquid material into fibers, which are then collected on the collector plate. To study the effect of the applied voltage on the nanofiber characteristics, a PVA:EXT (in situ) solution of 8% concentration was prepared and a range of spinning voltages were used ranging from 16 to 21 kV, as shown in Figure 2a–f. At a voltage of 16 kV,

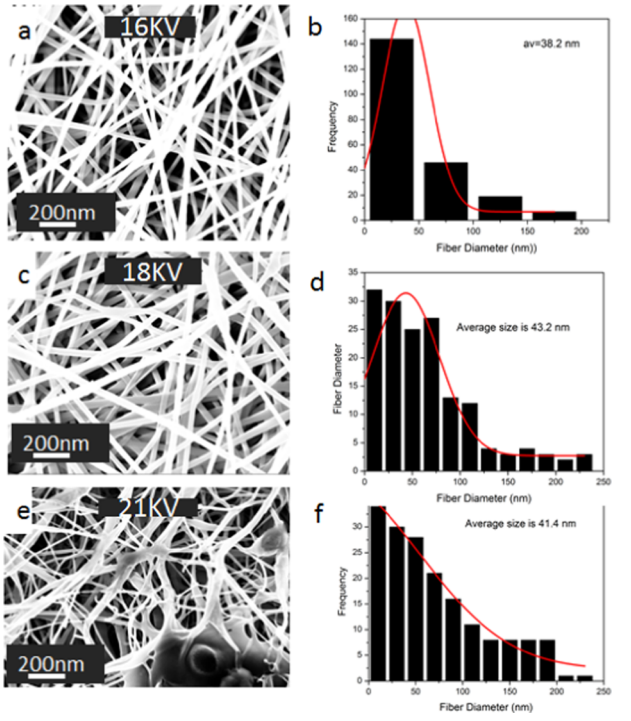

Figure 2. Scanning electron microscopy (SEM) images of 8% PVA:EXT nanofibers with the effect of voltages of (a) 16 kV, (c) 18 kV, and (e) 21 kV; solution flow rate of 1 mL/h, and the tip-to-collector distance of 12 cm. Their corresponding fiber diameter distribution histograms are shown in (b), (d), and (f).

nanofibers of PVA:EXT were smooth with no beads, and this voltage was ideal for fiber formation in all categories of material combinations. The diameter of the nanofibers in both PVA:EXT ranged between 35 and 80 nm, and there was a narrow diameter distribution, as shown in Figure 2a,b. As the voltage was increased to 18 kV, these properties changed, whereas incidences of bead formation were observed and the formed nanofibers generally appeared with fiber diameter inconsistency as well as increase in the average fiber diameter. The range of nanofiber diameter in both cases at 18 kV was found to be between 14 and 179 nm, which was nearly double the size of the fibers obtained at voltage 16 kV, as shown in Figure 2c,d. Moreover, as the voltage was increased further to 21 kV (as shown in Figure 2e), the fiber diameter was increased and there was a problem of wider diameter distribution (Figure 2f) as well as incidences of electric discharge. These results were consistent with the findings of Zhao et al. on the morphology of electrospun polyacrylamide nanofibers. Diameters of nanofibers for all parameters were analyzed using Image J analysis software and plotted by using Microsoft Origin lab software version 8.5.

In addition, the solution flow rate had a remarkable impact on the properties of the formed nanofibers, especially bead formation control. Composites were prepared and subjected to a constant voltage of 16 kV and the tip-to-collector distance of 12 cm while adjusting the solution flow rate from 0.8 to 1.2 mL/h. SEM images in Figure 3 reveal the extent of the impact

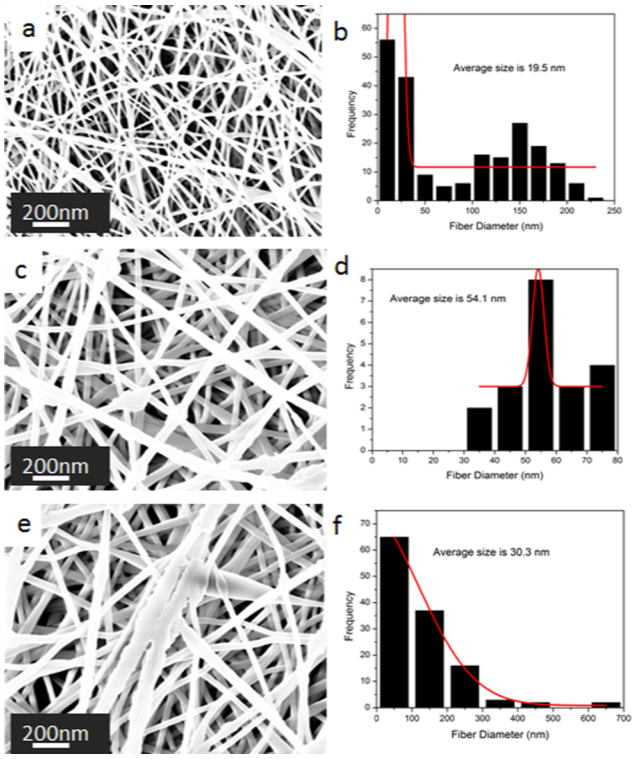

Figure 3. SEM images of PVA:EXT nanofibers with the effect of the solution flow rates of (a) 0.8 mL/h, (c) 1 mL/h, and (e) 1.2 mL/h at 16 kV and a tip-to-collector distance of 12 cm. Their corresponding fiber diameter distribution histograms are shown in (b), (d), and (f).

of solution flow rate on the formed nanofibers. When the solution flow rate was reduced to 0.8 mL/h, there was a shift in the fiber inconsistence and bead formation in both cases. At a solution flow rate of 1 mL/h, fiber formation was uninterrupted and the fibers were smooth with negligible levels of dropping (as shown in Figure 3a). On the other hand, when the solution flow rate was raised to 1.2 mL/h, there were challenges similar to those associated with low solution flow rate, as shown in Figure 3e.

Moreover, the concentration of the solution is one of the key factors, which determines the morphology of fibers that can be obtained by electrospinning. The influence of the PVA:EXT concentration on nanofiber formation is shown in the SEM images in Figure 4a,c,e,g. It was observed that the formation of smooth beadless fibers increases on increasing the concentration of the solution. At a concentration of 6% of PVA:EXT, fibers break along with beads, which however improved to smooth beadless fibers upon increasing the concentration to 8%. Moreover, as the concentration increased to 10% (SEM image in Figure 4e), fiber entanglement was observed, and at the concentration of 12%, ribbonlike structures were formed (SEM image in Figure 4g). All of these changes equally affected the fiber diameters, which increased as a result from 34

DOI: 10.1021/acsomega.9b00204
ACS Omega 2019, 4, 8778–8785

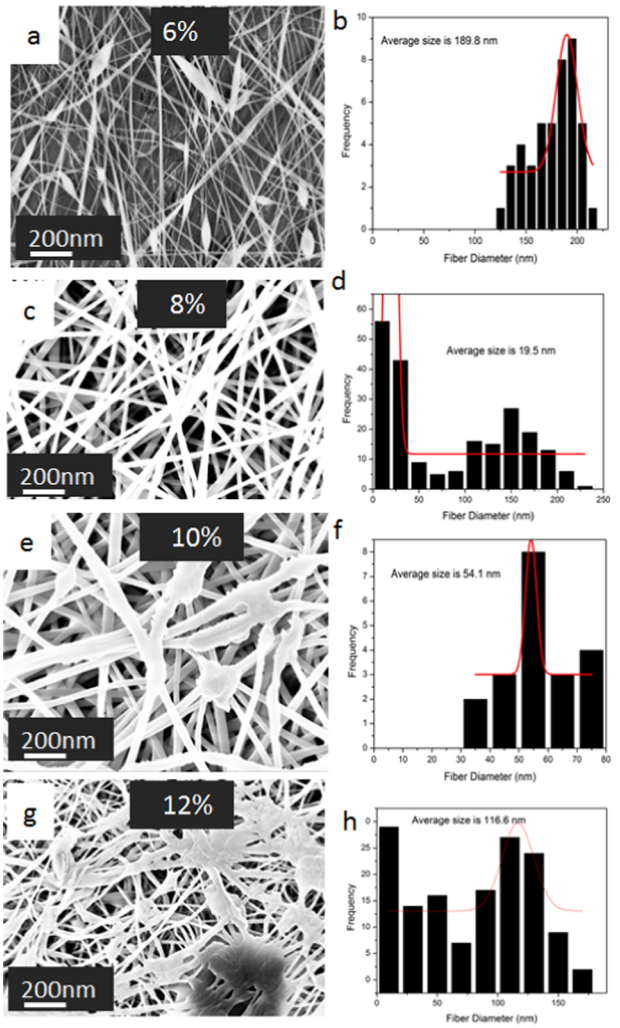

Figure 4. SEM images of PVA: EXT nanofibers electrospun at solution flow rate of 1mL/hour and applied voltage of 16kv from PVA solutions of concentration (w/w): (a) 6%, (c) 8%, (e) 10%, and (g) 12%. Their corresponding fiber diameter distribution histograms are shown in (b), (d), (f), and (h).

nm for 6% to over 100 nm for 12%, as shown in Figure 4b,d,f,h.

The lower concentration of the polymer was insufficient to maintain a stable jet from the tailor cone to the plate collector, and the breaks that resulted led to the formation of beads, as shown in the SEM micrographs in Figure 4a for PVA:EXT. This low concentration is associated with the increased surface tension, which cannot be overcome by the electrostatic forces because of the low chain entanglement in the solution and high solvent ratio in the solution. Yuan et al. attributed this scenario to the lower viscosity and conductivity of the material at a lower concentration as compared to higher concentrations. Thus, in the current work, we have also observed that the viscosity of the solution increased upon increasing the concentration of PVA:DBP/PVA:EXT as shown in the Supporting Information (Figure S12).

These morphological changes in the nanofibers are consistent with the findings made by Xu et al. and Yuan et al. although with slight differences, which arose due to current inconsistencies, molecular weight differences in chitosan, and also disparities in syringe pump efficiency.

2.3. Determination of Swelling and Weight Loss Percentages for Composite Nanofibers. The previously prepared polymer composite nanofibers (non-cross-linked) were tested for their swelling and weight loss percentages to determine their water absorption capacity and degradability. For comparison, we have also used cross-linked nanofibers made of the same components as the non-cross-linked ones. Figure 5 shows the high swelling capacity of all samples, with more emphasis on the cross-linked PVA:EXT:CS showing the highest value, while there was a decrease in weight loss percentage for all samples but was more obvious for PVA:EXT:CS, particularly the cross-linked nanofibers.

Based on these results, one can see that cross-linking of the composite nanofibers resulted into high swelling capacity and low weight loss. This might possibly be due to the fact that cross-linking of nanofibers might strengthen the interfiber bonding through either physical interaction or chemical groups (hydrogen bonding) introduced by glutaraldehyde. For swelling behavior, the presence of PVA, which is hydrophilic, possibly increases the capacity of the fibers to take up water. Moreover, introduction of amine groups from chitosan and glutaraldehyde enhances the water uptake behavior of the nanofibers. These results were in agreement with the findings of Kouchak et al., who studied water preservability but using PVA-based nanofibers for tissue engineering.[20] The principle of weight loss and swelling ability is very important for the nanofibers whose purposed application involves absorption of molecules while maintaining their intergrity. It is worth mentioning that the composite nanofibers (non-cross-linked) were selected for the antibacterial studies.

2.4. Chemical Analysis. *2.4.1. Fourier Transform Infrared (FTIR) Spectroscopy Analysis.* There was little chemical difference between the distilled and crude extracts of BP with hydroxyl and C−H group peaks at 3406 and 3412 cm^{-1} and mild primary amine and amide group peaks at 2900 and 1568 cm^{-1}, respectively (Figure 6). CS and PVA showed peaks of hydroxyl and primary amine groups (Figure 6A). Addition of chitosan to PVA:EXT showed changes in the chemical properties by the notable shifts in OH interactions and CN, NH, and C−X groups, as shown in Figure 6B.

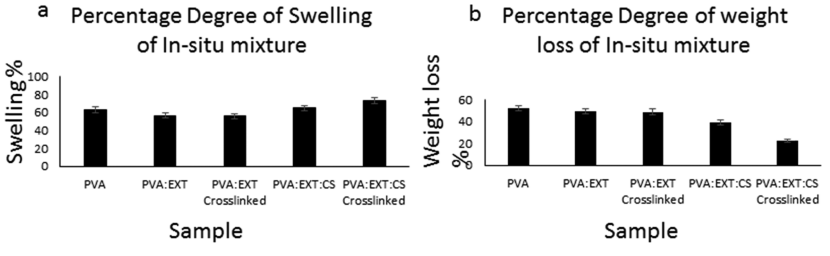

Figure 5. Immersion test: (a) swelling capacity and (b) weight loss of the PVA-, EXT-, and CS-derived nanofibers.

DOI: 10.1021/acsomega.9b00204
ACS Omega 2019, 4, 8778−8785

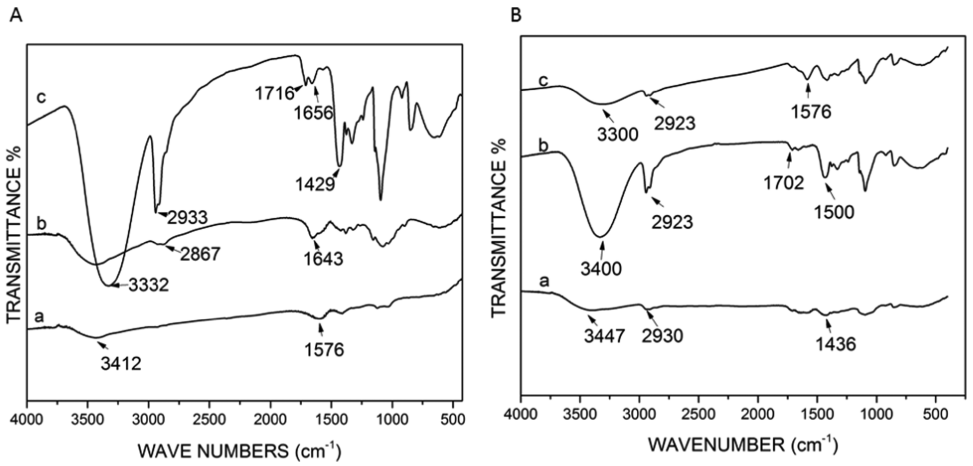

Figure 6. FTIR charts for (A) (a) crude extract of BP, (b) CS, and (c) PVA and (B) (a) PVA, (b) PVA:EXT (in situ), and (c) PVA:EXT:CS (in situ).

When PVA was mixed with the extract and CS, there was a shift in the peaks, especially in the OH stretching region at 3447 cm^{-1}. There is also a shift in the NH region and intensification at the region of O−H bending and C−O stretching, as shown in Figure 6B,a−c. It was observed that significant chemical changes occurred when PVA was dissolved in the crude extract of BP, as shown in Figure 6B. One such notable observation was the change in the OH bonds. OH bonds were strong in the PVA alone; however, when combined with the extract of BP, the intensity of OH groups reduced. Cross-linking nanofibers resulted in changes in both structural and chemical behaviors of the nanofibers. Physical SEM image analysis revealed structural changes in the nanofiber morphology and bonding between glutaraldehyde hydrogen groups and the surface groups on the fibers, as shown in Figure 7.

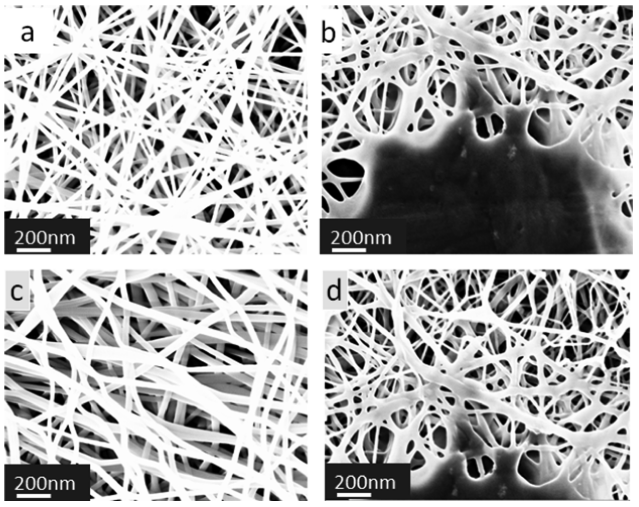

Figure 7. SEM images of (a) non-cross-linked PVA:EXT:CS, (b) cross-linked PVA:EXT:CS, (c) non-cross-linked PVA:EXT, and (d) cross-linked PVA:EXT.

FTIR spectroscopy analysis of the cross-linked nanofibers reveals significant chemical changes on interaction between glutaraldehyde and the composites (PVA, PVA:EXT (in situ and ex situ), and PVA:DBP (in situ and ex situ)) with a shift in peaks in the fingerprint region as can be seen in Figure S8 in the Support Information.

2.5. Antibacterial Testing. The antibacterial effect of the composite non-cross-linked nanofibers was evaluated using colony forming unit (CFU) enumeration. This method determines the number of viable bacterial cells in a sample following incubation. *Escherichia coli* and *Staphylococcus aureus* colonies were counted, and the standard deviation of the triplicates was calculated.

Although PVA is not known to have antibacterial effect as a polymer, it showed limited effect against *E. coli* and insignificant results against *S. aureus*. On the other hand, CS showed moderate activity against both *E. coli* and *S. aureus* (55.6 and 40%, respectively) (Figure 8A).

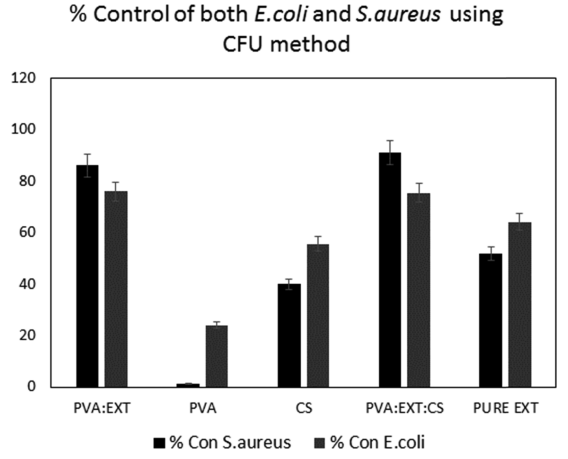

Figure 8. Percentage inhibition of both *S. aureus* and *E. coli* in the presence of PVA:EXT, PVA, CS, PVA:EXT:CS (in situ), and pure extract of BP at the seventh dilution.

BP composite nanofibers (i.e., PVA:EXT and PVA:EXT:CS) formed both in situ and ex situ (see the Supporting Information figure) were effective against both *E. coli* and *S. aureus* owing to the combined effect of the crude extract of BP and CS. PVA:EXT inhibited 75.9 and 86% growth of *E. coli* and *S. aureus*, respectively, while PVA:EXT:CS inhibited 75.4 and 91% growth of *S. aureus*, as shown in Figure 8. Crude extract of BP composite nanofibers (PVA:EXT) exhibited a higher antibacterial activity when compared with the distilled BP (see Supporting Information figures). The crude extract of BP alone showed a remarkably higher activity; 64 and 51.7%

DOI: 10.1021/acsomega.9b00204
ACS Omega 2019, 4, 8778−8785

against *E. coli* and *S. aureus*, respectively. Pure distillate of BP showed lower antibacterial activity against *E. coli* (60%) and *S. aureus* (40%), respectively. Statistical analysis of the antibacterial assay was performed using one-way analysis of variance. Such statistical analysis revealed a significant enhancement in the antibacterial activity using PVA:EXT and PVA:EXT:CS ($P < 0.05$).

The minimum inhibition concentration (MIC) for the PVA:EXT, PVA:EXT:CS, and pure extract of BP was obtained to be 10 mg/mL, while the minimum bactericidal concentration was between 10 and 20 mg/mL. The log reduction is summarized in Table 1.

Table 1. In Situ Composite Nanofibers and Their Log Reduction Values

	log reduction value	
sample (in situ)	*E. coli*	*S. aureus*
PVA:EXT	1.05	0.99
PVA:EXT:CS	0.99	0.77
pure EXT	0.94	0.6

Similar work carried out by Nguyen et al. using polylactic acid and CS nanofibers revealed high and sustained antibacterial activity of the nanofibers. The increase in the antibacterial effects at the nanoscale is linked to the changes in the chemical properties that occur with reduction in size, thus exposing chemically active groups that interact with the cell membrane of bacteria.

This nanocomposite system and also the enhanced antibacterial activity of the BP extract in the nanofiber delivery system have not been reported in the literature. This is therefore an important discovery for biomedical applications, especially for wound healing applications.

3. CONCLUSIONS

Pure CS nanofibers could not be electrospun from pure CS dissolved in 1% acetic acid. This was due to the high viscosity and tension created by the polycationic nature of CS. CS nanofibers were produced when a lower amount of CS was blended with PVA and CS interacted with PVA polymers, forming H-bonds and thus reducing the polyelectrolyte effect. A blend of PVA−CS with a higher amount of PVA produced a nearly defect-free mesh of nanofibers with fiber diameters ranging from 30 to 150 nm. To form nanofibers containing the BP extract, the blend had to have a higher amount of PVA and the fiber diameter was found to be in the range between 25 and 200 nm. Although the crude extract of BP resulted in challenges during electrospinning and dissolution of PVA due to the presence of tannins, it provided smoother nanofibers than the other category. Composites of either crude extract or distilled BP on combining with CS produced mixed results. While it was easier to form electrospun nanofibers with PVA:DBP:CS, it was difficult to get substantial fibers with PVA:EXT:CS. In the cases where combinations

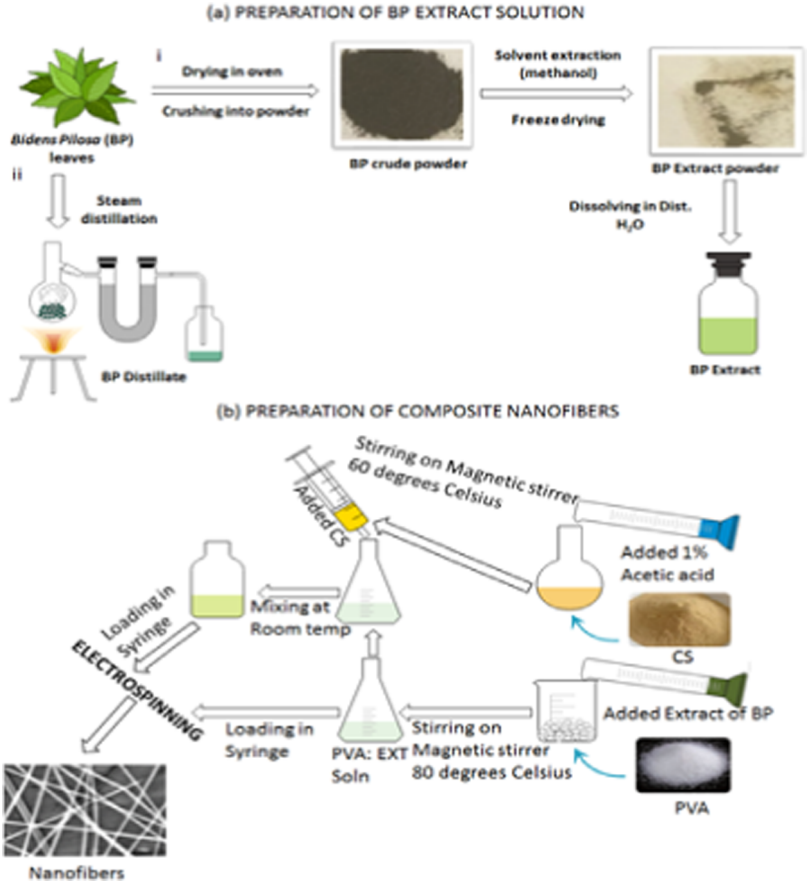

Figure 9. Schematic representation of (a) preparation of the BP crude (i) and distilled (ii) extracts. (b) Preparation of composite nanofibers. The images were created using the mind graph and e-draw software.

DOI: 10.1021/acsomega.9b00204
ACS Omega 2019, 4, 8778−8785

with CS yielded nanofibers, the amount of PVA in the mixture played a crucial role. Increasing the amount of PVA in the mixture reduced the formation of beads and thus produced smooth fibers. Blended solutions were best electrospun within 24 h of mixing to achieve smooth fiber formation. The mixing has to be followed with a rest period of 4 h to allow any hanging particles to fully settle. When the antibacterial tests of these different blends of composites were carried out against *E. coli* and *S. aureus*, it was determined that nanofiber composites (PVA:DBP, PVA:DBP:CS, PVA:EXT, and PVA:EXT:CS) showed higher antibacterial properties (74 and 83, 69.8 and 81.4, 75.9 and 86, and 75.4 and 91% against *E. coli* and *S. aureus*, respectively) than their parental form. The broad spectrum of the antibacterial activity of BP and CS composite nanofibers can be applied in the biomedical industry to counter the increased threat of antibacterial resistance.

4. MATERIALS AND METHODS

4.1. Materials. PVA (MW 125 000, 20−98% hydrolysis) was purchased from Sigma-Aldrich, Europe. CSs (cg1600 with 76% degree of deacetylation and cg400 with 84.8% degree of deacetylation) were purchased from Primex ehf (Chitoclear, Iceland). BP was purchased from SEFA organic extracts Kampala Uganda, and Difco LB agar medium and Difco LB (Luria-Bertani) broth media were purchased from Becton Dickinson Company. The bacterial strains used in this study were *S. aureus* ATCC 6538 and *E. coli* ATCC 8739.

4.2. Synthesis Procedures. *4.2.1. Synthesis of Composite Nanofibers.* Figure 9 is a schematic representation illustrating the preparation steps of BP crude/distilled extracts (EXT) and the composite nanofibers of PVA mixed with BP EXT and with chitosan (CS). First, PVA, PVA:DBP, and PVA:EXT (PVA in EXT and PVA in DBP) with percentages ranging from 7 to 12% were prepared by two methods: (a) in situ by dissolving PVA powder (7.0−15.0 g) into BP solution (w/v) and (b) ex situ volumetric addition of PVA solution (prepared by dissolving PVA (7.0−15.0 g) powder in deionized water) to different solution volumes of the two BP separately at a ratio of 2:1 up to 5:1 (v/v), respectively.

After the successful preparation of PVA:EXT solutions, the composites of PVA:EXT:CS were prepared by mixing PVA, PVA:EXT (in situ), and PVA:EXT (ex situ) with CS at a ratio ranging from 2:1 up to 5:1 (v/v) and stirred at room temperature for 4 h.

Each of the prepared solutions was electrospun into nanofibers using an electrospinner (E-Spin Tech, India) connected to a syringe pump and high-voltage supply (Gamma high-voltage power supply). Solutions from the above composites were loaded into 10 mL syringes and mounted onto the pump, which was connected to the electrospinner through a silicon tube. A solution flow rate ranging between 0.3 and 1.6 mL/h was applied while being connected to the high applied voltage ranging between 10 and 28 kV. The nanofibers were collected on aluminum foil grounded on the metallic collector located 10−20 cm away from the spinneret.

4.3. Characterization. *4.3.1. Morphological Characterization. 4.3.1.1. Scanning Electron Microscopy (SEM).* In this characterization, SEM (FESEM, Leo Supra 55—Zeiss Inc., Germany), field emission electron microscope was employed to determine the morphological characteristics of the nanofibers. Samples for imaging were prepared by cutting 2 cm^2 of the aluminum foil containing the fibers and put on the stage for SEM imaging. The FESEM was operated at a working distance of 3 mm and probe current of 4 kV. In addition, a bench-top SEM was used for EDX analysis to study the chemical elements that are contained in the composite materials.

4.3.2. Chemical Characterization. Chemical characterization was carried out by Fourier transform infrared spectroscopy (FTIR) (Nicolet 380-Thermo Scientific). This technique was used to determine the chemical composition of the materials before and after blending to understand the interactions that existed when blended and also the functional groups and characterizing their properties. Samples used in the FTIR analysis included both powder and nanofibers forms. A sample of both cases was mixed with KBr pellets and ground. The mixture was ground at a ratio of 1:0.2 (KBr/sample, respectively) because KBr was already thick as it is required that a small amount of the sample is to be added (according to Beer Lambert's law). The samples were then compressed to form discs and then were placed in the FTIR instrument and analyzed.

4.3.3. Physical Characterization. Physical properties including swelling and weight loss were tested following the Moradkhannejhad et al. procedure with slight modification.[11]

Cross-linked and non-cross-linked nanofibers were immersed in a phosphate buffer solution (PBS) with a pH of 7.4 and were incubated at 37 °C for 24 h to determine the swelling capability and thus the ability to absorb exudates with ease. Similarly, to determine the degree of degradability of the nanofibers and thus their stability in various applications, weighted nanofiber sheets were immersed in PBS for 24 h followed by wiping off the surface PBS and vacuum-drying the nanofibers for 3 h. Non-cross-linked nanofibers are known to disintegrate fast in an aqueous environment than the cross-linked nanofibers. Cross-linking of the nanofibers was done by placing the nanofibers above glutaraldehyde in a desiccator for 12 h. Cross-linking can also be done after withdrawing them from water; then, the nanofiber films were rinsed off the surface PBS using soft white tissue and weighed to get the weight (Wt). Furthermore, they were dried in a vacuum oven for 5 h and then weighed to get WD.[11] The percentages of degree of swelling and weight loss were obtained from the two equations mentioned below, eqs 1 and 2.[11]

$$\text{degree of swelling} = \frac{(\text{Wt} - W_0)}{W_0} \times 100 \quad (1)$$

$$\text{weight loss \%} = \frac{(W_0 - \text{WD})}{W_0} \times 10 \quad (2)$$

Wt is the weight after immersion in PBS, W_0 is the dry weight before immersion in PBS, and WD is the weight after drying the immersed fibers.[11]

4.3.4. Antibacterial Testing. The antibacterial property of the nanocomposite fibers was determined by colony forming unit (CFU) enumeration. This method gives information on the number of viable bacteria following incubation with a bactericidal agent. The colonies formed are counted, and percentage inhibition is determined. Luria-Bertani (LB) broth and agar were prepared as per the manufacturer instruction. The two bacterial strains used in this test were *E. coli* (top 10 MC1061) representing the Gram-negative and *S. aureus* (ATCC 6538) representing Gram-positive bacteria. PVA:EXT nanofibers were weighed, standardized at 5 mg, and sterilized under a UV lamp for 2 h. Media containing *E. coli* and *S. aureus*

DOI: 10.1021/acsomega.9b00204
ACS Omega 2019, 4, 8778−8785

(2 mL, 0.1 OD) with the samples (in triplicates) were incubated for 24 h at 37 °C. As a control, 2 mL of bacterial culture and 2 mL of blank media (uncultured), to eliminate contamination errors, were incubated at the same temperature and for the same duration. A parallel experiment involving addition of 5 mg/mL nanofiber samples into blank media to ascertain the sterility of the samples was also carried out. After 24 h, the samples were serially diluted (to 1×10^{-6} and 1×10^{-7}) and 50 μL of the suspension was plated on LB agar plates, incubated at 37 °C overnight, and the CFUs were counted the next day. Because of the large cell count, we diluted the cultures with fresh sterilized media to reach the following dilutions, 1×10^{-6} and 1×10^{-7}, by adding 50 μL of the diluted bacterial media into 450 μL of fresh media to allow colony counting.

Equation 3 was used to calculate the control percentage[18]

$$\% \text{ control} = \frac{(\text{positive control} - \text{sample})}{\text{positive control}} \times 100 \quad (3)$$

The minimum inhibition concentration (MIC) was also determined. Log reduction was calculated using eq 4[21]

$$\log \text{reduction} = \log A/\log B \times 100 \quad (4)$$

■ ASSOCIATED CONTENT

Supporting Information

The Supporting Information is available free of charge on the ACS Publications website at DOI: 10.1021/acsomega.9b00204.

(PDF)

■ AUTHOR INFORMATION

Corresponding Author

*E-mail: wael_mamdouh@aucegypt.edu.

ORCID

Rania Siam: 0000-0002-2879-6368

Wael Mamdouh: 0000-0003-0642-1992

Notes

The authors declare no competing financial interest.

■ ACKNOWLEDGMENTS

The authors acknowledge the financial support received from the American University in Cairo (AUC) through student and Faculty Support Research Grants.

■ REFERENCES

(1) Davies, J.; Davies, D. Origins and Evolution of Antibiotic Resistance. *Am. Soc. Microbiol.* **2010**, *74*, 417−433.

(2) Tagliabue, A.; Rappuoli, R. Changing Priorities in Vaccinology: Antibiotic Resistance Moving to the Top. *Front. Immunol.* **2018**, *9*, No. 1068.

(3) Spellberg, B.; Guidos, R.; Gilbert, D.; Bradley, J.; Boucher, H.; Scheld, W.; Bartlett, J.; Edwards, J. The Epidemic of Antibiotic-Resistant Infections: A Call to Action for the Medical Community from the Infectious Diseases Society of America. *Clin. Infect. Dis.* **2008**, *46*, 155−64.

(4) Högberg, L. D.; Heddini, A.; Cars, O. The Global Need for Effective Antibiotics: Challenges and Recent Advances. *Trends Pharm. Sci.* **2010**, *31*, 509−515.

(5) Whitman, A.; Lambert, P.; Dyson, O.; Akula, S. Applications of Nanotechnology in the Biomedical Sciences: Small Materials, Big Impacts, and Unknown Consequences. In *Emerging Conceptual, Ethical and Policy Issues in Bionanotechnology*; Springer, 2008; pp 117−130.

(6) Tocco, I.; Zavan, B.; Bassetto, F.; Vindigni, V. Nanotechnology-Based Therapies for Skin Wound Regeneration. *J. Nanomater.* **2012**, 1−11.

(7) Feng, C.; Khulbe, K. C.; Matsuura, T.; Tabe, S.; Ismail, A. F. Preparation and Characterization of Electro-Spun Nanofiber Membranes and Their Possible Applications in Water Treatment. *Sep. Purif. Technol.* **2013**, *102*, 118−135.

(8) Mo, A.; Liao, J.; Xu, W.; Xian, S.; Li, Y.; Bai, S. Preparation and Antibacterial Effect of Silver−hydroxyapatite/Titania Nanocomposite Thin Film on Titanium. *Appl. Surf. Sci.* **2008**, *255*, 435−438.

(9) Jia, Z.; Li, Q.; Yang, Y.; Wang, L.; Guan, Z. In *Preparation and Properties of Poly (Vinyl Alcohol) Nanofibers by Electrospinning*, IEEE International Conference on Solid Dielectrics, Winchester, U.K., July 8−13, 2007.

(10) Monogue, M.; Thabit, A.; Hamada, Y.; Nicolau, D. Antibacterial Efficacy of Eravacycline In Vivo against Gram-Positive and Gram-Negative Organisms. *Antimicrob. Agents Chemother.* **2016**, *60*, 5001−5005.

(11) Moradkhannejhad, L.; Abdouss, M.; Nikfarjam, N.; Mazinani, S.; Sayar, P. Electrospun Curcumin Loaded Poly(Lactic Acid) Nanofiber Mat on the Flexible Crosslinked PVA/PEG Membrane Film. *Fibers Polym.* **2017**, *18*, 2349−2360.

(12) Subbiah, T.; Bhat, G. S.; Tock, R. W.; Parameswaran, S.; Ramkumar, S. S. Electrospinning of Nanofibers. *J. Appl. Polym. Sci.* **2005**, *96*, 557−569.

(13) Opanasopit, P.; Ruktaananchal, U.; Suwantong, O.; Panomsuk, S.; Ngawhirunpat, T.; Sittisombut, C.; Suksamran, T.; Supaphol, P. Electrospun poly (vinyl alcohol) fiber mats as carriers for extracts from the fruit hull of mangosteen. *J. Cosmet. Sci.* **2008**, *59*, 233−242.

(14) Zhao, Y.; Zhou, Y.; Wub, X.; Wang, L.; Xua, L.; Wei, S. A Facile Method for Electrospinning of Ag Nanoparticles/Poly (Vinyl-alcohol)/Carboxymethyl-Chitosan Nanofibers. *Appl. Surf. Sci.* **2012**, *258*, 8867−8873.

(15) Peresin, M.; Habibi, Y.; Zoppe, J.; Pawlak, J.; Rojas, O. Nanofiber Composites of Poly(vinyl Alcohol) and Cellulose Nanocrystals: Manufacture and Characterization. *Biomacromolecules* **2010**, *11*, 674−681.

(16) Li, C.; Fu, R.; Yu, C.; Li, Z.; Guan, H.; Hu, D.; Zhao, D.; Lu, L. Silver Nanoparticle/Chitosan Oligosaccharide/Poly(Vinyl Alcohol) Nanofibers as Wound Dressings. *Int. J. Nanomed.* **2013**, *8*, 4131−4145.

(17) Jana, S.; Florczyk, S.; Leung, M.; Zhang, M. Designing of Chitosan-Based Scaffolds for Biomedical Applications. *J. Mater. Chem.* **2012**, *22*, 6291−6299.

(18) Unnithan, A. R.; Barakatb, N.; Pichiah, T.; Gnanasekarane, G.; Nirmala, R.; Cha, Y.-S.; Junge, C.-H.; El-Newehy, M.; Kimb, H. Y. Wound-Dressing Materials with Antibacterial Activity from Electrospun Polyurethane−dextran Nanofiber Mats Containing Ciprofloxacin HCl. *Carbohydr. Polym.* **2012**, *90*, 1786−1793.

(19) Bartolome, A. P.; Villaseñor, I.; Yang, W. *Bidens pilosa* L. (Asteraceae): Botanical Properties, Traditional Uses, Photochemistry, and Pharmacology. *J. Evidence-Based Complementary Altern. Med.* **2013**, *2013*, 1−50.

(20) Kouchak, M.; Ameri, A.; Naseri, B.; Boldaji, S. Chitosan and poly(vinyl alcohol) composite films containing nitrofurazone; preparation and evaluation. *Iran. J. Basic Med. Sci.* **2014**, *17*, 14−20.

(21) MacGowan, A.; Rogers, C.; Holt, A.; Wootton, M.; Bowker, K. Assessment of Different Antibacterial Effect Measures Used in in Vitro Models of Infection and Subsequent Use in Pharmacodynamic Correlations for Moxifloxacin. *J. Antimicrob. Chemother.* **2000**, *46*, 73−78.

DOI: 10.1021/acsomega.9b00204
ACS Omega 2019, 4, 8778−8785